PHOTOCATALYTIC DEGRADATION OF PARACETAMOL USING HIGHLY ORDERED TIO_2 NANOTUBE ARRAYS PREPARED BY ELECTROCHEMICAL ANODIZATION

Ashega Sherly. R[1], Padma C.M[2], Henry Raja D[3]

[1]Research scholar, Reg No. 19213282132013 Department of Physics and Research centre, Women's Christian College, Nagercoil, Tamilnadu, India.
[2]Department of Physics and Research centre, Women's Christian College, Nagercoil, Tamilnadu, India.
[3]Department of physics and Research centre, Scott Christian College (Autonomous), Nagercoil, Tamilnadu, India.
(Affiliated to Manonmaniam Sundaranar University, Tirunelveli, Tamilnadu, India)

Email: [1]ashega95@gmail.com

Article History: **Received:** 19.01.2022 **Revised:** 04.02.2022 **Accepted:** 12.03.2022

Abstract

This research looks into the photocatalytic degradation of paracetamol using anodized TiO_2 nanotubes. The electrolyte containing 0.2 wt% NH_4F, 2 vol% H_2O, and ethylene glycol was employed to fabricate TiO_2 nanotubes. The dimension of the anodized TiO_2 nanotubes was controlled by increasing the anodization potential from 12 V to 60 V. The formation of anatase phase was confirmed by X-ray diffraction studies and it also demonstrated the influence of the anodization potential on the crystallite size. Surface dimensions, surface roughness, porosity, and aspect ratio of the nanotubes were analysed by Field-emission scanning electron microscopy. UV-DRS and photoluminescence spectroscopy were used to investigate the TiO_2 nanotubes' optical characteristics. The bandgap values computed from the Tauc plot demonstrate how the anodization potential affects the bandgap of the material. The lowest band gap (2.89 eV) was observed for the samples anodized at 12V. The effect of UVC and UVA light sources (11 Watt) during degradation and initial concentration of paracetamol were studied. Even with a relatively low-power UV radiation, 15.5% of paracetamol conversion was observed in 180 min.

Keywords: TiO_2 nanotube, Paracetamol degradation, XRD, Band gap, UV-DRS.

DOI: 10.53555/ecb/2022.11.03.16

1. Introduction

Titanium dioxide (TiO_2) has been identified as a potential photocatalyst due to its outstanding charge transport capabilities in photocatalytic organic pollutant removal and photocatalytic hydrogen production. However, the ineffective use of visible light and poor adsorption behaviour represent significant barriers to the use of TiO_2 photocatalysts [1]. TiO_2 is primarily utilized as a food colouring agent, a white pigment in paints and pharmaceutical products, a sunscreen to filter UV rays, and in cosmetics, polymers, ceramics, and other industries because of these qualities. It demonstrates promising uses in nano sensors, solar cells, UV filters, batteries, and biological fields, such as genetic engineering and photodynamic therapy for cancer [2]. For the fabrication of TiO2, various methods like hydrothermal, sol-gel, co-precipitation, sputtering, and anodization [3]–[6] have been reported. Additionally, different morphologies including nanoflowers, nanospheres, nanorods, nanowires, and nanotubes have also been reported[7], [8]. Among the following methods, the anodization method is preferred by researchers because of its unique morphology, which facilitates better ion transportation, and its large surface area, which provides better reactivity. Several alterations to the tube geometry have been developed due to its flexibility in adjusting anodization parameters without the need for expensive machinery, including bamboo-shaped nanotubes, branched nanotubes, single-walled or double-walled nanotubes, and nanotubes that are spaced apart. [9]–[11].

Paracetamol is an analgesic and antipyretic medication most widely utilised worldwide. Pharmaceutical wastes reach water bodies through the immediate disposal of excess medications in residences, human excretion, and insufficient effluent treatment. The widespread presence of pharmaceutical waste in aquatic ecosystems has prompted serious concerns about human health and the environment. Pharmaceutical pollution can harm aquatic life, cause genotoxicity, and affect the endocrine system. Paracetamol degradation can be achieved by physicochemical processes, such as sand filtration, membrane separation, activated carbon, chlorination, and oxidation. Biological processes for the degradation of paracetamol include anaerobic treatment, aerobic treatment, activated sludge (AS) processing, membrane bioreactors (MBR), and phytoremediation. The disadvantage of using these methods is that the pollutant will not be eliminated completely; instead, only the phase of the pollutant will be changed [12], [13].

The current study deals with the fabrication of TiO_2 nanotubes with a fixed ammonium fluoride (NH_4F) concentration, deionized water (H_2O), and ethylene glycol (EG), but with different anodization potentials, varying from 12 to 60 V. The effect of anodization potential on the structure and dimensions of the nanotubes, the change of the band gap, and the successful usage of fabricated nanotubes as a photocatalyst to degrade aquoeus paracetamol contaminants in the presence of UVC and UVA radiation were studied.

Experimental Details

Fabrication of Catalyst

Titania (TiO_2) nanotubes were fabricated using an electrochemical anodization process that employs a two-electrode arrangement. Before anodization, the samples are washed in a sequence of ethanol, acetone, and deionized water for approximately 10 minutes to eliminate impurities, and then dried. Titanium foil (thickness: 0.25mm; 99.7% purity; Sigma-Aldrich, USA) was cut into 1cm x 3cm pieces and used as the working electrode and platinum (Thickness: 0.025mm; 99.9% purity; Sigma-Aldrich, USA) was used as

the cathode. Experiments were carried out at six different voltages (12, 20, 30, 40, 50 and 60V) for 1 hour using a DC power source (skyking, model no. 6005) at room temperature. The anode and cathode were separated by a distance of approximately 2 cm. Ethylene glycol ($C_2H_6O_2$ - 99.8% purity; Sigma-Aldrich, USA) was the primary component of the electrolyte with 0.3 wt% (in mass) NH_4F (98.0% purity; Sigma-Aldrich, USA) and 2% (in volume) H_2O. Anodized Ti foil was annealed for 1 hour at 430°C in a muffle furnace to achieve the crystalline phase in static air. X-Ray diffractometer (D8 advance) was used to determine the crystallinity, phase formation, and lattice parameters. A Field Emission Scanning Electron Microscope (Carl Zeiss, SUPRA 55VP) was used to detect the surface image of the anodized Ti foil, and ImageJ software was used to calculate the average diameter and length. A UV-VIS spectrophotometer (Shimadzu UV-3600 plus) and a Photo-Luminescence spectrophotometer (Varian Cary Eclipse) were used to measure the absorbance and emission properties of the materials.

Photocatalytic Study

The photocatalytic degradation of paracetamol was carried out in a reactor under UVC and UVA irradiation. A 0.4 g/L starting concentration, 0.1 g/L paracetamol, and a 3 cm x 1 cm TiO_2 nanotube photocatalyst were utilized. The photocatalyst was 10 cm distant from the light source. For 30 minutes, the photocatalyst was immersed in paracetamol solution to establish adsorption-desorption equilibrium. The degradation was carried out for 3 hours, and every 30 minutes, 2 ml of paracetamol solution was withdrawn and the residual concentration was determined using a UV-Vis spectrometer (SHIMADZU, UV 3600 PLUS).

2. Results and Discussion

X-ray diffraction analysis

The fig 1 shows the XRD patterns of TiO_2 anodized at different voltages and annealed at 430ºC. The pattern shows reflection of anatase peaks at 2θ= 25.27, 37.84, 38.05, 70.711 which are assigned to the planes (1 0 1), (0 0 4), (1 1 2) and (2 2 0) of TiO_2 (JCPDS # 00-021-1272), respectively. The nanotubes anodized at lower voltages have few titanium peaks in them and anatase peaks (1 1 2), (2 2 0) are present. When the voltage is increased to 20 V, anatase peaks are formed at 2θ = 25.27 and 37.9 which are assigned to planes (1 0 1) and (0 0 4) respectively. When the anodizing voltage was 60 V, the intensity of the titanium peaks and other anatase peaks decreased and only the anatase phase (0 0 4) is dominant.

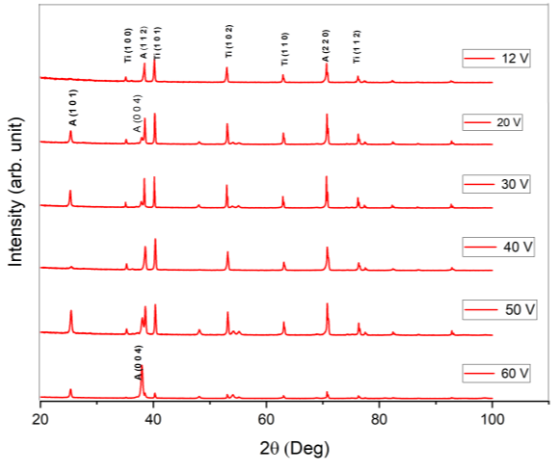

Fig 1 XRD patterns of TiO_2 nanotube arrays calcined at 430ºC

To obtain more structural information about anodized TiO_2 nanotubes, structural parameters such as crystalline size and d spacing are calculated. The anodized TiO_2 nanotubes have a tetragonal structure and it is confirmed by comparing the 2θ of XRD data with the standard data file (reference code JCPDS# 00-021-1272). The crystalline size can be calculated from the Debye-Scherrer equation[14]. Our results indicate that the crystallite size was dependent on the anodization potential. Table 1 shows the calculated value of d spacing, standard value of d spacing, FWHM and crystallite size of the samples fabricated at different voltages. From table 1 we can observe that sample fabricated at 12V anodization potential shows smallest crystallite size and as we increase the anodization potential, the crystallite size is observed to increase initially and then decreases.

Table 1. Size of crystallites calculated from XRD data

VOLTAGE (V)	2θ (deg)	d- spacing (Å)		FWHM (deg)	CRYSTALLITE SIZE (D) (nm)
		$d_{calculated}$	$d_{standard}$		
12	38.42	2.340	2.3320	0.374	23.5
20	38.51	2.334	2.3320	0.2502	35.1
30	38.37	2.343	2.3320	0.3235	27.2
40	38.57	2.331	2.3320	0.1724	51
50	38.59	2.330	2.3320	0.2147	40.9
60	37.97	2.3669	2.3780	0.2839	30.9

FESEM analysis

Using field emission scanning electron microscopy, the morphology of the resultant TiO_2 nanotubes was determined. The fractured spaces of the samples were used to create the cross-sectional image. Fig 2 shows top-view photographs of samples created by electrochemical oxidation of titanium at various voltages, Fig 3 shows cross-sectional images and Table 2 shows tube dimensions (diameter, length, and wall thickness), porosity, roughness factor and aspect ratio based on FESEM images.

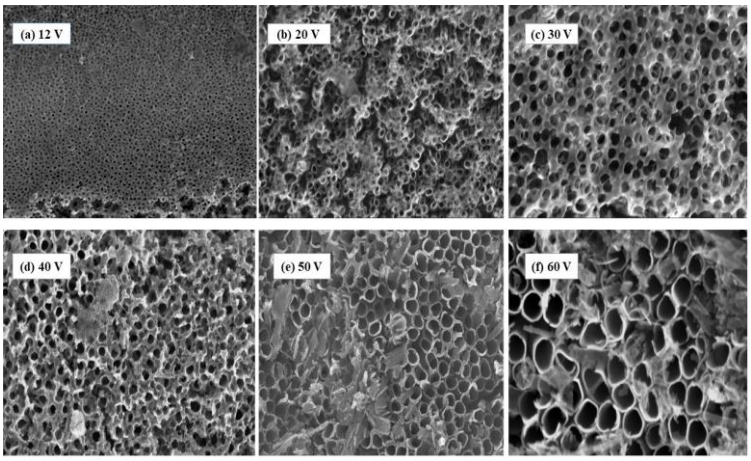

Fig 2 Top view FESEM images of titania nanotube arrays anodized at different voltages (a) 12 V, (b) 20 V, (c) 30 V, (d) 40 V, (e) 50 V, (f) 60 V

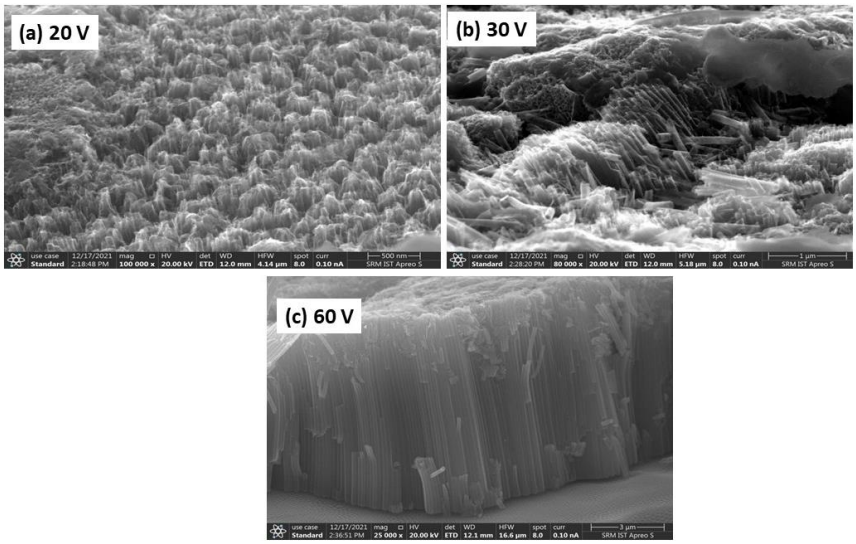

Fig 3 Cross-sectional FESEM images of titania anodized at different voltages (a) 20 V, (b) 30 V, (c) 60 V

Table 2. Architectural characteristics of TIO_2 nanotube arrays under different conditions.

Conditions	Diameter (nm)	Wall thickness (nm)	Length (nm)	Porosity (%)	Surface Roughness	Aspect ratio (length/Diameter)
12 V/ 1 h	18	4.11	-	21	0.0321	-
20 V/ 1 h	23.541	5.412	141	51	0.1777	5.989
30 V/ 1 h	51.04	6	703	68	0.1040	13.77
40 V/ 1 h	89.268	8.7	-	72	0.0624	-
50 V/ 1 h	101.138	9.828	-	72	0.0551	-
60 V/ 1 h	122.315	10.716	4340	74	0.0460	35.48

According to earlier studies, an electrolyte based on ethylene glycol tends to produce nanotubes that are smoother and more uniform, which leads the diameter of the TiO_2 nanotube to increase as the anodization voltage rises.[15]. By keeping other anodization parameters constant and changing the anodization, the pore diameters shows a clear variation which were calculated from FE-SEM image. Increasing the voltage from 12 to 60 V, the pore diameter is shown to increase approximately from 18 to 122.315 nm, and this was calculated using ImageJ software. The thickness of the nanotube walls also increased from 4.11 to 10.716 nm. At 12 V, the surface has pores of various diameters ranging from 6 to 30.18 nm. This is because the applied anodization potential directly affects the rate of field-assisted oxidation and dissolution reactions that occur during nanotube production. At lower applied voltages, the electric field is low causing smaller pits resulting in smaller diameter tubes. The electrochemical etching of fluoride ions into the pits is also small causing shorter nanotubes. At higher applied voltages, higher electric field causes bigger pits with thicker oxide layer and electrochemical

etching also increases causing longer tubes [6]. The amplitude of the applied voltage directly affects the nano-tube diameter at the tube mouth and bottom. Ku et al. reported that the inner diameter and the length of the titania nanotubes were increased linearly with an increase in anodization potential from 38 to 177 nm and 420 to 1910 nm in fluoride containing electrolytes [16]. Etching of fluoride ions and electrochemical oxidation plays an important role in tube formation. The anodization potential can be increased up to a certain stage until the electrochemical oxidation rate and the chemical dissolution rate reach a dynamic equilibrium [17]. The nanotube diameters and wall thickness depend on the applied voltage as follows:

$$d(nm) = kV \quad (1)$$

$$l(nm) = hV \quad (2)$$

where V, l, and d stand for the anodization voltage, length, and diameter of the nanotubes, respectively. Additionally, *k* and *h* represent the diameter and wall thickness growth coefficients of the nanotubes. According to the data of the above table, *k* and *h* are estimated to be 1.582 (nm/V) and 0.2342 (nm/V) respectively. The porosity and the roughness factors were calculated and listed in table 2 [18], [19]. According to table 2, anodization potential significantly affects the porosity and the roughness factor of the titania nanotubes. The porosity is increased from 21 to 74 % and the aspect ratio also found to be increased at higher voltage.

UV – DRS analysis

The optical band gap values were calculated for each modified catalyst according to the Kubelka – Munk model of $(\alpha h\nu)^{1/2}$ vs $h\nu$ from the UV- vis- DRS transmittance spectra in the 200 – 600 nm range (fig 4a). DRS is a very helpful optical test, and by evaluating its reflectance and absorption spectra, one can learn more about the material's electronic transitions. Initially, the sample anodized at 12 V provided a band gap (energy difference between the top of the valence bond and the bottom of the conduction band) of 2.89 eV, and increasing the voltage to 20 V yielded a band gap of 3.07 eV. The band gaps of the samples anodized at 30 and 40 V were 3.13 eV and 2.93 eV, respectively, and the band gap of the sample anodized at 50 V was 3 eV. The sample anodized at 60 V had a band gap of 3.1 eV. Table 3 displays the calculated band gap and R^2 values. The calculated band gap values (Eg) are less than the optical band gap (Eg(bulk)) of bulk TiO_2 at room temperature, which is 3.2 eV. Figure 4b depicts the reflection spectra of samples made at various anodization voltages. The samples anodized from 20 to 50 V exhibit a redshift, while the sample anodized at 60 V exhibits a minor blueshift. Low band gap of 2.89 eV was observed for samples anodizes at 12 V.

Table 3. Band gap energy of titania nanotubes anodized at different potentials.

Voltage (V)	**Band–gap (eV)**	**R^2**
12	2.89	0.9973
20	3.07	0.9945
30	3.13	0.9956
40	2.93	0.9941
50	3.00	0.9956
60	3.10	0.9979

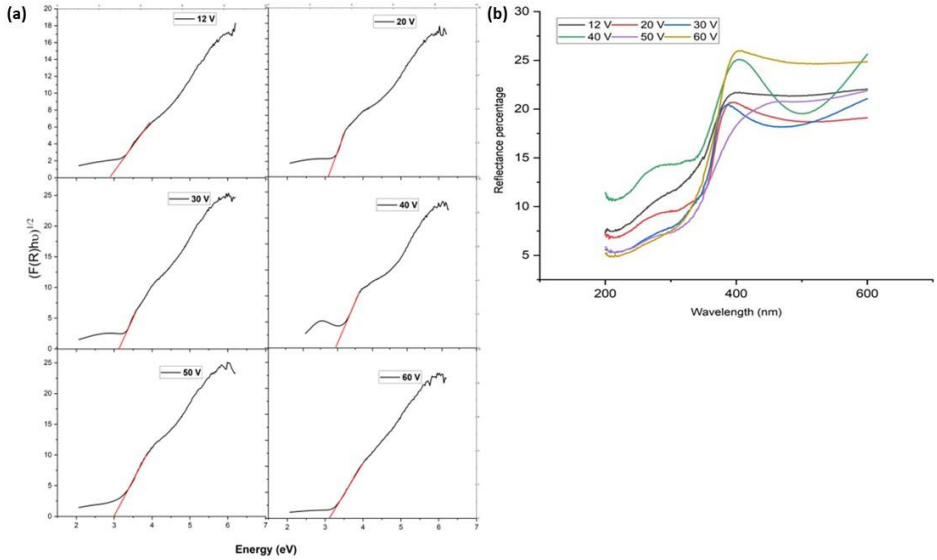

Fig 4 (a)The plots of $(\alpha h\nu)^{1/2}$ versus (eV) graph for the samples anodized at different anodization voltages (b) UV-Vis-DRS spectrum of all synthesized titania nanotubes anodizes at different voltages

Photoluminescence Spectroscopy

Photoluminescence (PL) is a crucial and contactless optical technique to assess the purity and crystalline quality of materials for energy devices and to pinpoint specific impurities. The photoluminescence (PL) spectra of titania nanotubes anodized at different voltages ranging from 12 to 60 V in the wavelength range of 300 to 600 nm are shown in Fig 5. In the extensive range of spectra, the spectrum displays a number of distinct bands. These bands' locations and relative intensities are nearly equal and independent of the average internal diameter of titania nanotubes. A significant PL emission peak is observed at ~361 nm for all the samples and the bandgap was calculated which is approximately ~3.25 eV. The remaining peaks formed show the oxygen vacancies and the free excitations on the surface of the titania nanotubes.

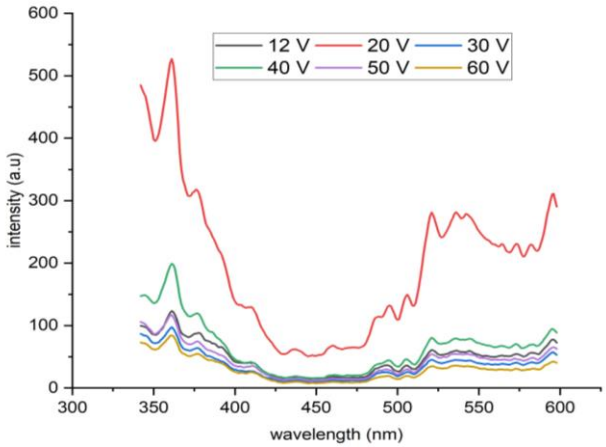

Fig 5 Photoluminescence spectra of titania nanotubes at different voltages in the range of 300–600 nm

Photocatalytic Activity Results

Effect of Type of UV Radiation

The samples fabricated with anodization potential of 12 V possessed lower band gap of 2.89 eV compared with other samples. Therefore, it was used for the photocatalytic degradation of paracetamol. A fixed quantity of paracetamol was degraded in the presence of two different types of UV light, UVC (11-Watt) and UVA (11-Watt) for 180 minutes, to measure the photocatalytic activity of the fabricated TiO_2 nanotubes. Light illumination during the degradation process plays a crucial part in photodegradation process. The energy of the illuminated light should be equal to or greater than the bandgap of the photocatalyst. The wavelength ranges of the UVA and UVC radiations were 400-315 nm and 280-100 nm respectively. UVC radiation possesses higher energy than UVA radiation. Under UVC radiation illumination, 15.5% degradation of paracetamol was observed. A degradation of only 0.9% was observed when illuminated with UVA radiation. Bozkurt Cirak et al. and Phong et al. also reported similar results. Photodegradation of RhB and effluents dissolved in organic matter was performed under the illumination of different UV radiations, and maximum degradation was obtained when illuminated with UVC radiation[20],[21] The results obtained are listed in Table 4.

Table 4. Photocatalytic study of TiO_2 based photocatalyst

Material	Pollutant	Light source	% degradation	Reference
ZnO-TiO_2	RhB	UVA	22	[20]
		UVC	100	
TiO_2	Effluents dissolved organic matter	UVA	45.1	[21]
		UVC	83	
TiO_2	Paracetamol	UVA	0.9	Present work
		UVC	15.5	

The degradation of paracetamol can be explained by the electron-hole generation model. When a photon with an energy larger than or equal to the material's band gap strikes the catalyst's surface, electrons from the valence band migrate to the conduction band. As a result, holes formed in the valence band. •OH and superoxide radicals (O2 •) are formed when the electron-hole pair combines with hydroxyl radicals or water species. These species degrade in the presence of ultraviolet (UV) radiation. Figure 8 shows the photocatalytic activity of the prepared TiO_2 nanotubes in the presence of UVC radiation. When the photocatalyst was exposed with UVC radiation, the degradation efficiency increased because UVC radiation has more energy than UVA radiation, allowing more electrons to be excited from the valence band to the conduction band. As a result, more electron-hole pairs are generated, resulting in a higher degradation efficiency. The experimental data were found to approximately fit the zeroth-order kinetic model (fig 6). The rate constant was 0.00081 $gL^{-1}min^{-1}$ (R^2 = 0.92). Zero order kinetics indicates that the rate of the reaction is independent of the concentration of the reactants

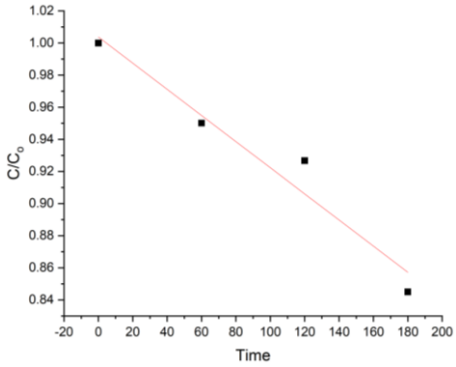

Fig 6 Photocatalytic activity of prepared TiO_2 nanotubes for the degradation of paracetamol.

Effect of Initial Concentration

The effect of initial paracetamol concentration was studied by illumination with UVA radiation for 180 min. Degradation of paracetamol at two initial concentrations namely 0.1 g/L and 0.4 g/L was studied. When the initial concentration decreased, an increase in the degradation was observed. When the initial concentration was 0.1 g/L, 3% degradation was observed. When the initial concentration was 0.4 g/L, a 0.9% degradation was observed. Vaiano et al. reported a decrease in photodegradation when the initial concentration of paracetamol was increased from 25 mg/L to 50 mg/L[22]. The reason for the very low degradation at higher concentrations can be attributed to the low energy radiation and high concentration of paracetamol, which results in a reduced number of electron-hole pairs, leading to decreased degradation. The reason for the increase in photodegradation efficiency with a decrease in the initial concentration of paracetamol is that, for fixed dimensions of the photocatalyst and UV radiation, the holes and radicals produced were constant. When the concentration of the pollutant is increased, the photons emitted by UV light are not sufficient to maintain the same photocatalytic reaction as the previous one. This leads to a decrease in the efficiency.

Stability

The reusability of the photocatalysts is another important aspect. The photocatalytic stability of the TiO_2 photocatalyst under UVC radiation, with 0.4 g/L initial paracetamol concentration of is shown in fig 7. The photocatalyst retained 41.2%, 30.9%, and 17.4% efficiencies after the second, third, and fourth cycles, respectively.

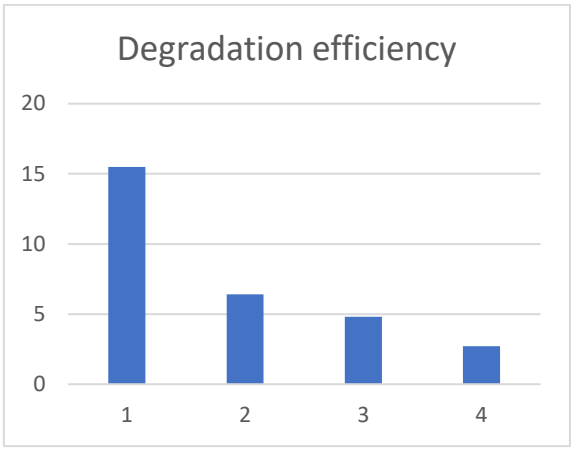

Fig 7 The reusability of the photocatalyst in the degradation of paracetamol with initial concentration of 0.4 g/L in the presence of UVC light illumination

3. Conclusion

In this study, TiO_2 nanotube arrays were fabricated at different anodization potentials viz 12V, 20V, 30V, 40V, 50V and 60V and structural, morphological, and optical characterizations were performed using XRD, FESEM, photoluminescence and UV-DRS analysis. The samples fabricated at a potential of 12 V possessed a low band gap compared with other samples and hence were used for the photocatalytic study of paracetamol in the presence of UV radiation. The effects of UV illumination, the initial concentration of paracetamol, and the stability of the photocatalyst were studied. Paracetamol degradation of 15.5 % was observed when illuminated with UVC radiation, and when illuminated with UVA radiation, only 3% was observed. This is due to the low energy of the UVA radiation. The effect of the initial paracetamol concentration was also studied. When the initial concentration increased, the degradation decreased. This is because when the concentration of paracetamol increased, the radicals formed upon illumination with UV radiation were not sufficient to degrade the paracetamol components. The stability of the photocatalysts was also investigated. The photocatalyst retained 41.2%, 30.9%, and 17.4% efficiencies after the second and fourth cycles, respectively. This study concludes that TiO_2 can be effectively used as a photocatalyst for paracetamol degradation. Even at the low-power illumination of UVC (11-Watt) radiation, 15.5% degradation efficiency was obtained in 180 min.

4. Reference

1. J. H. Lee, S. J. Mun, S. Y. Lee, and S. J. Park, “Promoted charge separation and specific surface area via interlacing of N-doped titanium dioxide nanotubes on carbon nitride nanosheets for photocatalytic degradation of Rhodamine B,” Nanotechnol Rev, vol. 11, no. 1, pp. 1592–1605, Jan. 2022, doi: 10.1515/ntrev-2022-0085.
2. H. Nura, S. G. Abdu, A. Shauibu, and M. S. Abubakar, “Electronic Band Structure and Optical Properties of Titanium Dioxide,” Science World Journal, vol. 14, no. 3, p. 2019, [Online]. Available: www.scienceworldjournal.org
3. J. Lee, D. H. Kim, S. H. Hong, and J. Y. Jho, “A hydrogen gas sensor employing vertically aligned TiO2 nanotube arrays prepared by template-assisted method,” Sens Actuators B Chem, vol. 160, no. 1, pp. 1494–1498, Dec. 2011, doi: 10.1016/j.snb.2011.08.001.

4. L. Dreesen, J. F. Colomer, H. Limage, A. Giguère, and S. Lucas, "Synthesis of titanium dioxide nanoparticles by reactive DC magnetron sputtering," Thin Solid Films, vol. 518, no. 1, pp. 112–115, Nov. 2009, doi: 10.1016/j.tsf.2009.06.044.
5. K. Manjunath, L. S. Reddy Yadav, T. Jayalakshmi, V. Reddy, H. Rajanaika, and G. Nagaraju, "Ionic liquid assisted hydrothermal synthesis of TiO2 nanoparticles: photocatalytic and antibacterial activity," Journal of Materials Research and Technology, vol. 7, no. 1, pp. 7–13, Jan. 2018, doi: 10.1016/j.jmrt.2017.02.001.
6. M. A. Behnajady, H. Eskandarloo, N. Modirshahla, and M. Shokri, "Investigation of the effect of sol-gel synthesis variables on structural and photocatalytic properties of TiO2 nanoparticles," Desalination, vol. 278, no. 1–3, pp. 10–17, Sep. 2011, doi: 10.1016/j.desal.2011.04.019.
7. Z. H. Ren et al., "Au nanoparticles embedded on urchin-like TiO2 nanosphere: An efficient catalyst for dyes degradation and 4-nitrophenol reduction," Mater Des, vol. 121, pp. 167–175, May 2017, doi: 10.1016/j.matdes.2017.02.064.
8. Q. E. Zhao, W. Wen, Y. Xia, and J. M. Wu, "Photocatalytic activity of TiO2 nanorods, nanowires and nanoflowers filled with TiO2 nanoparticles," Thin Solid Films, vol. 648, pp. 103–107, Feb. 2018, doi: 10.1016/j.tsf.2018.01.004.
9. M. Motola et al., "Comparison of photoelectrochemical performance of anodic single- and double-walled TiO2 nanotube layers," Electrochem commun, vol. 97, pp. 1–5, Dec. 2018, doi: 10.1016/j.elecom.2018.09.015.
10. S. Ozkan, A. Mazare, and P. Schmuki, "Critical parameters and factors in the formation of spaced TiO2 nanotubes by self-organizing anodization," Electrochim Acta, vol. 268, pp. 435–447, Apr. 2018, doi: 10.1016/j.electacta.2018.02.120.
11. J. Zhang, W. Huang, K. Zhang, D. Li, H. Xu, and X. Zhu, "Bamboo shoot nanotubes with diameters increasing from top to bottom: Evidence against the field-assisted dissolution equilibrium theory," Electrochem commun, vol. 100, pp. 48–51, Mar. 2019, doi: 10.1016/j.elecom.2019.01.019.
12. K. Ikehata, N. Jodeiri Naghashkar, and M. Gamal El-Din, "Degradation of aqueous pharmaceuticals by ozonation and advanced oxidation processes: A review," Ozone: Science and Engineering, vol. 28, no. 6. pp. 353–414, Dec. 01, 2006. doi: 10.1080/01919510600985937.
13. A. Nikolaou, S. Meric, and D. Fatta, "Occurrence patterns of pharmaceuticals in water and wastewater environments," in Analytical and Bioanalytical Chemistry, Feb. 2007, pp. 1225–1234. doi: 10.1007/s00216-006-1035-8.
14. M. Meftahi, S. H. Jafari, and M. Habibi-Rezaei, "Fabrication of Mo-doped TiO2 nanotube arrays photocatalysts: The effect of Mo dopant addition time to an aqueous electrolyte on the structure and photocatalytic activity," Ceram Int, vol. 49, no. 7, pp. 11411–11422, Apr. 2023, doi: 10.1016/j.ceramint.2022.11.340.
15. R. V. Chernozem, M. A. Surmeneva, and R. A. Surmenev, "Influence of Anodization Time and Voltage on the Parameters of TiO2 Nanotubes," in IOP Conference Series: Materials Science and Engineering, Institute of Physics Publishing, Mar. 2016. doi: 10.1088/1757-899X/116/1/012025.
16. Y. Ku, Z.-R. Fan, Y.-C. Chou, and W.-Y. Wang, "Characterization and Induced Photocurrent of TiO[sub 2] Nanotube Arrays Fabricated by Anodization," J Electrochem Soc, vol.

157, no. 6, p. H671, 2010, doi: 10.1149/1.3384659.
17. H. Ennaceri et al., "Effect of morphology on the photoelectrochemical activity of TiO2 self-organized nanotube arrays," Catalysts, vol. 10, no. 3, Mar. 2020, doi: 10.3390/catal10030279.
18. J. V. Pasikhani, N. Gilani, and A. E. Pirbazari, "The effect of the anodization voltage on the geometrical characteristics and photocatalytic activity of TiO2 nanotube arrays," Nano-Structures and Nano-Objects, vol. 8, pp. 7–14, Oct. 2016, doi: 10.1016/j.nanoso.2016.09.001.
19. T. Hoseinzadeh, Z. Ghorannevis, M. Ghoranneviss, A. H. Sari, and M. K. Salem, "Effects of various applied voltages on physical properties of TiO2 nanotubes by anodization method," Journal of Theoretical and Applied Physics, vol. 11, no. 3, pp. 243–248, Sep. 2017, doi: 10.1007/s40094-017-0257-9.
20. B. Bozkurt Çırak et al., "Synthesis and characterization of ZnO nanorice decorated TiO2 nanotubes for enhanced photocatalytic activity," Mater Res Bull, vol. 109, pp. 160–167, Jan. 2019, doi: 10.1016/j.materresbull.2018.09.039.
21. D. D. Phong and J. Hur, "Non-catalytic and catalytic degradation of effluent dissolved organic matter under UVA- and UVC-irradiation tracked by advanced spectroscopic tools," Water Res, vol. 105, pp. 199–208, Nov. 2016, doi: 10.1016/j.watres.2016.08.068.
22. V. Vaiano, O. Sacco, and M. Matarangolo, "Photocatalytic degradation of paracetamol under UV irradiation using TiO2-graphite composites," Catal Today, vol. 315, pp. 230–236, Oct. 2018, doi: 10.1016/j.cattod.2018.02.002.